JOURNAL OF GUIDANCE, CONTROL, AND DYNAMICS
Vol. 19, No. 2, March–April 1996

Design and Robustness Analysis of Gain-Scheduled Control System for Parabolic Flight

F. Amato,* G. Ambrosino,† and M. Mattei‡
University of Naples "Federico II," Napoli 80125, Italy
and
L. Verde§
Centro Italiano Ricerche Aerospaziali, Capua 80143, Italy

The problem of designing a flight control system for the tracking of parabolic trajectories to guarantee microgravity conditions within the aircraft cabin is considered. The proposed control action consists of two parts. The first one is a feedforward control guaranteeing good tracking of the desired parabola in the absence of environmental disturbances. The second part is a gain-scheduled output feedback to counteract possible misalignments between the desired output trajectory and the actual one. An estimation of the maximum output displacement in the presence of uncertainties and disturbances (wind gusts) is carried out. Simulation results are provided for a remotely piloted vehicle.

Nomenclature

A = wing aspect ratio
C_D = drag coefficient
C_L = lift coefficient
C_m = pitch moment coefficient
c = reference chord, m
g = acceleration of gravity, m/s^2
I_y = pitching moment of inertia, kgm^2
m = mass of the airplane, kg
q = pitch rate, deg/s
$\bar{q}$ = dynamic pressure ($:= \frac{1}{2}\rho v_a^2$), N/m^2
S = reference area, m^2
s, z = center of gravity coordinates in a coordinate system fixed on the Earth, m
T = thrust, N
u_g = horizontal component of wind gust or turbulence, m/s
v = aircraft speed relative to ground, m/s
v_a = aircraft speed relative to wind-based reference frame $\{:=\sqrt{[(v+u_g)^2 + w_g^2]}\}$, m/s
w_g = vertical component of wind gust or turbulence, m/s
α = angle of attack deg
α_a = angle of attack ($:= \alpha + \arctan\{[w_g/(v+u_g)]\}$), deg
γ = flight-path angle ($:= \theta - \alpha$), deg
δ_e = elevator deflection, deg
θ = pitch angle, deg
ρ = air density, kg/m^3

I. Introduction

MICROGRAVITY experiments are usually carried out in Space Shuttles and, consequently, are very expensive. To reduce their costs, various alternatives to obtain microgravity conditions have been proposed. Among these, parabolic flights on commercially available aircrafts with free-floating laboratories seem to be one of the most promising because of the good compromise between realization cost, microgravity level, and time duration of the experiment (about 30 s).

To avoid collisions of the free-floating laboratory with the internal walls of the cabin, it is necessary to force the aircraft to follow the parabolic trajectory of a body subjected only to the gravity force. Because of the presence of aerodynamic forces and environmental disturbances, such as wind gusts and turbulence, and the high accuracy level required during the maneuver, an automatic flight control system (AFCS) can considerably increase the percentage of successful flights with respect to those obtainable by an experienced human pilot. Based on these considerations, the Centro Italiano Ricerche Aerospaziali (Italian Aerospace Research Center; CIRA) has been carrying out research in developing a remotely piloted vehicle (RPV) that should allow some microgravity experiments.[1] The role of CIRA in this program is to investigate and design an AFCS for the parabolic flights of the RPV. This problem has been already investigated in the literature. In Ref. 2 the authors proposed a control algorithm based on the online evaluation of the control inputs by means of a nonlinear optimization technique. An alternative control law, which makes use of the dynamic inversion technique previously developed in Refs. 3 and 4, is proposed in Ref. 5. A problem of these techniques is that they require the use of a powerful computer because of their burdensome computational load.

A remarkable simplification of the control problem can be obtained by assuming that the desired parabola to be tracked differs slightly from a fixed one, hereinafter called the nominal parabola. This nominal parabola is the solution to an offline optimization problem in which the time duration of the parabolic flight is maximized by taking into account constraints on the maximum load factor and the maximum thrust of the aircraft. As a matter of fact, the desired parabola to be tracked depends on the actual initial speed vector of the airplane, i.e., the speed vector at the end of the pull-up phase.[1] Because of the presence of disturbances during the pull-up phase, the initial speed vector and, consequently, the desired parabola may differ from the nominal one.

We propose a control scheme based on two combined control actions: 1) a feedforward control, evaluated online by means of some simple explicit formulas based on the desired parabola and 2) a gain-scheduled linear output feedback control, designed offline, to nullify possible misalignments, resulting from environmental disturbances, between the desired position of the aircraft and the actual one.

The design of the gain-scheduled feedback controller is carried out by considering only some flight conditions of the plane along the nominal parabola. Since, as already stated, the desired parabola may differ from the nominal one, a robustness analysis of the closed-loop system needs to be addressed before the overall scheme could be considered as a practical system for parabolic flights. This analysis, together with a performance analysis to estimate the maximum wind

Received May 31, 1995; revision received Oct. 6, 1995; accepted for publication Oct. 13, 1995.

*Assistant Professor, Dipartimento di Informatica e Sistemistica, Via Claudio 21.
†Professor, Dipartimento di Informatica e Sistemistica, Via Claudio 21.
‡Ph.D. Student, Electrical Engineering, Dipartimento di Informatica e Sistemistica, Via Claudio 21.
§Head, Flight Mechanics and Control Group, Via Maiorise.

gust allowable during the parabola, is carried out by a procedure based on the approach proposed in Ref. 6.

The paper is organized as follows: Sec. II contains the formulation of the control problem. The design of the controller is developed in Sec. III, and in Sec. IV the robustness analysis is carried out. Finally, the effectiveness of the proposed control scheme and the weak conservativeness of the proposed analysis technique are shown by numerical simulations in Sec. V.

II. Aircraft Model and Control Objectives

In this study the microgravity laboratory is assumed to be free to move within the aircraft cabin from the initial time t_0 at which the microgravity experiment starts. Moreover, without loss of generality, we assume that at the time t_0 the laboratory center of mass coincides with that of the airplane. Finally, for the sake of simplicity of presentation, only the more interesting longitudinal motion control problem of the aircraft is considered. By assuming a wind axes reference frame for the velocity and an inertial frame for the position, the equations of the longitudinal motions of a rigid aircraft, symmetrical with respect to the vertical plane and flying at small sideslip and roll angles, can be written as[7]

$$\dot{\alpha} = -\frac{\bar{q}S}{mv}C_L + q + \frac{g}{v}\cos\gamma - \frac{T\sin\alpha}{mv} \tag{1a}$$

$$\dot{q} = (\bar{q}Sc/I_y)C_m \tag{1b}$$

$$\dot{v} = -\frac{\bar{q}S}{m}C_D - g\sin\gamma + \frac{T\cos\alpha}{m} \tag{1c}$$

$$\dot{\gamma} = \frac{\bar{q}S}{mv}C_L - \frac{g}{v}\cos\gamma + \frac{T\sin\alpha}{mv} \tag{1d}$$

$$\dot{s} = v\cos\gamma \tag{1e}$$

$$\dot{z} = v\sin\gamma \tag{1f}$$

The aerodynamic coefficients C_L, C_D, and C_m generally depend nonlinearly on α_a, q, v_a, δ_e, and on the external disturbances u_g and w_g via α_a and v_a.

By defining the state vector $\boldsymbol{x} := (\alpha\ q\ v\ \gamma\ s\ z)^T$, the control vector $\boldsymbol{u} := (\delta_e\ T)^T$, the output vector $\boldsymbol{y} := (v\ \gamma\ s\ z)^T$, and the disturbance vector $\boldsymbol{\mu} := (u_g\ w_g)^T$, Eqs. (1) can be rewritten in the following compact form:

$$\dot{\boldsymbol{x}} = \boldsymbol{f}(\boldsymbol{x}, \boldsymbol{u}, \boldsymbol{\mu}) \tag{2a}$$

$$\boldsymbol{y} = (\boldsymbol{O}\ \boldsymbol{I}_4)\boldsymbol{x} := \boldsymbol{C}\boldsymbol{x} \tag{2b}$$

By assuming that the available volume for the microgravity laboratory within the aircraft is a sphere of radius M, during the time interval $[t_0, t_f]$ in which the microgravity experiment takes place, the controller task is the online determination of the control law $\boldsymbol{u}(\cdot)$ so as to avoid collisions between the microgravity laboratory and the walls of the aircraft cabin. This is a tracking problem in which the center of mass of the aircraft must follow the trajectory of the laboratory, i.e., the trajectory of a mass only subjected to the gravity force. By assuming, without loss of generality, $t_0 = 0$, $s(0) = 0$, $z(0) = 0$, and letting $v(0) = v_0$, $\gamma(0) = \gamma_0$, the desired output trajectory $\boldsymbol{y}_d(\cdot)$ is given by

$$\boldsymbol{y}_d(t) = \begin{pmatrix} v_d(t) \\ \gamma_d(t) \\ s_d(t) \\ z_d(t) \end{pmatrix} = \begin{pmatrix} \sqrt{(v_0\cos\gamma_0 - gt)^2 + (v_0\sin\gamma_0)^2} \\ \arctan\dfrac{v_0\cos\gamma_0 - gt}{v_0\sin\gamma_0} \\ v_0 t\cos\gamma_0 \\ v_0 t\sin\gamma_0 - 0.5gt^2 \end{pmatrix} \tag{3}$$

Note that $\boldsymbol{y}_d(\cdot)$ depends only on the initial speed vector of the aircraft $\boldsymbol{w}_d(0) := \boldsymbol{w}_0 = (v_0\ \gamma_0)^T$ in an inertial frame. In fact, this initial speed vector depends on the time histories of the control commands and of the environmental disturbances during the pull-up phase just preceding the parabolic flight.

The control commands in the pull-up phase can be computed off-line so as to maximize, in the absence of atmospheric disturbances, the time duration of the parabolic flight subjected to constraints on the maximum load factor and on the maximum thrust of the aircraft.[1] In this way the resulting nominal value $\boldsymbol{w}_{n0}$ of the speed vector at the end of the pull-up phase and the corresponding nominal parabola $\boldsymbol{y}_n(\cdot)$, obtained from Eq. (3) by replacing $\boldsymbol{w}_0$ with $\boldsymbol{w}_{n0}$, are known. Because of the presence of realistic atmospheric disturbances during the pull-up phase, we assume that the true initial speed vector $\boldsymbol{w}_0$ belongs to a known neighborhood of $\boldsymbol{w}_{n0}$, say, $\mathcal{W}_0$.

III. Proposed Control Technique

The control input $\boldsymbol{u}(\cdot)$ is determined as the sum of two actions: a feedforward action $\boldsymbol{u}_d(\cdot)$ and a feedback action $\boldsymbol{u}_{fb}(\cdot)$.

A. Feedforward Control

The feedforward part of the control law, namely, $\boldsymbol{u}_d(\cdot)$, has been chosen as the control function guaranteeing an optimal output tracking in the absence of external disturbances. It can be obtained as the solution of the following dynamic optimization problem.

Problem 1:

$$\min_{\boldsymbol{u}(\cdot)[0,t_f],\alpha_0,q_0} \int_0^{t_f} \left(\boldsymbol{e}_y^T\boldsymbol{Q}\boldsymbol{e}_y + \boldsymbol{u}^T\boldsymbol{R}\boldsymbol{u}\right) \mathrm{d}t \tag{4}$$

subject to

$$\dot{\boldsymbol{x}} = \boldsymbol{f}(\boldsymbol{x}, \boldsymbol{u}, \boldsymbol{0}), \qquad \boldsymbol{x}(0) = [\alpha_0\ q_0\ \boldsymbol{y}(0)]^T, \qquad \boldsymbol{y} = \boldsymbol{C}\boldsymbol{x}$$

where $\boldsymbol{e}_y := \boldsymbol{y} - \boldsymbol{y}_d$ and $\boldsymbol{Q}$ and $\boldsymbol{R}$ are suitable positive definite weighting matrices.

Note that the optimal values of the initial state variables α_0 and q_0 are determined together with the optimal control function $\boldsymbol{u}_d(\cdot)$ to minimize the performance index. The optimization over α_0 and q_0 is needed to obtain a desired state trajectory $\boldsymbol{x}_d(\cdot)$ that is also optimal with respect to the angular position of the aircraft expressed by the state variables $\alpha(t)$ and $q(t)$. Later in the paper we shall show that this optimization will also have benefits in the design of the feedback control law.

Unfortunately the numerical techniques previously proposed to solve this problem (e.g., Ref. 2) are computationally cumbersome and cannot be used online; therefore we propose an alternative algorithm to solve Problem 1, which is detailed in Appendix A.

B. Feedback Control

On the basis of the preceding discussion, once the initial speed vector $\boldsymbol{w}_0$ has been measured, the desired output trajectory $\boldsymbol{y}_d(\cdot)$ together with the control input $\boldsymbol{u}_d(\cdot)$ guaranteeing the best tracking of $\boldsymbol{y}_d(\cdot)$ can be computed. In practice, if just the feedforward control action is used because of 1) a possible initial displacement of the state variables $\alpha(t)$ and $q(t)$ with respect to their optimal values resulting from the solution of Problem 1 and 2) the presence of atmospheric disturbances (wind gusts) occurring during the parabola, a misalignment between the desired output trajectory and the actual one may occur; hence a feedback control action is needed.

We assume that the input disturbance belongs to the class of sudden wind gusts of short time duration occurring in the time interval $[0, t_f]$; to fix the ideas we assume that the disturbance is impulsive and occurs at the time $t = 0$, that is, $\boldsymbol{\mu}(t) = \boldsymbol{d}\delta(t)$, where $\delta(t)$ is the Dirac function. In this way both the uncertainty on $\alpha(0)$ and $q(0)$ (point 1) and the action of atmospheric disturbances (point 2) can be treated as an initial state displacement $\Delta\boldsymbol{x}_0 := \boldsymbol{x}(0) - \boldsymbol{x}_d(0)$.

To use one of the optimal control techniques, which seem to be well suited for the design of the feedback controller, we could linearize the aircraft model (2) around the desired state trajectory obtained by solving Problem 1. We would have

$$\Delta\dot{\boldsymbol{x}} = \left[\frac{\partial \boldsymbol{f}}{\partial \boldsymbol{x}}\right]_{\substack{\boldsymbol{x}=\boldsymbol{x}_d(\cdot)\\ \boldsymbol{u}=\boldsymbol{u}_d(\cdot)\\ \boldsymbol{\mu}=\boldsymbol{0}}} \Delta\boldsymbol{x} + \left[\frac{\partial \boldsymbol{f}}{\partial \boldsymbol{u}}\right]_{\substack{\boldsymbol{x}=\boldsymbol{x}_d(\cdot)\\ \boldsymbol{u}=\boldsymbol{u}_d(\cdot)\\ \boldsymbol{\mu}=\boldsymbol{0}}} \Delta\boldsymbol{u}$$

$$:= \tilde{\boldsymbol{A}}_d[\boldsymbol{x}_d(t), \boldsymbol{u}_d(t)]\Delta\boldsymbol{x} + \tilde{\boldsymbol{B}}_d[\boldsymbol{x}_d(t), \boldsymbol{u}_d(t)]\Delta\boldsymbol{u}$$

$$\Delta\boldsymbol{x}(0) = \Delta\boldsymbol{x}_0 \tag{5a}$$

$$\Delta\boldsymbol{y} = \boldsymbol{C}\Delta\boldsymbol{x} \tag{5b}$$

where

$$\Delta \boldsymbol{x}_0 = \begin{cases} [\Delta\alpha(0) \quad \Delta q(0) \quad \boldsymbol{0}]^T & \text{(6a)} \\ \tilde{\boldsymbol{B}}_\mu[\boldsymbol{x}_d(0), \boldsymbol{u}_d(0)]\boldsymbol{d} := \left[\dfrac{\partial \boldsymbol{f}}{\partial \boldsymbol{\mu}}\right]_{\substack{\boldsymbol{x}=\boldsymbol{x}_d(\cdot) \\ \boldsymbol{u}=\boldsymbol{u}_d(\cdot) \\ \mu=0}} (0)\boldsymbol{d} & \text{(6b)} \end{cases}$$

As previously stated, however, the exact desired state trajectory $\boldsymbol{x}_d(\cdot)$ and the optimal control $\boldsymbol{u}_d(\cdot)$ cannot be computed offline. Therefore, the matrices of the linearized model (5) are unknown.

The key consideration to overcome this difficulty consists in noting that by virtue of the Bellman optimality principle and the fact that in Problem 1 we make the solution independent on the initial value of the state variables α_0 and q_0, for each $t \in [0, t_f]$ the optimal solution of Problem 1 $[\boldsymbol{x}_d(t), \boldsymbol{u}_d(t)]$ depends only on $\boldsymbol{y}_d(0)$ and, therefore, because of Eq. (3), on $\boldsymbol{w}_d(0) = [v_d(0) \quad \gamma_d(0)]^T$ or equivalently on $\boldsymbol{w}_d(t) = [v_d(t) \quad \gamma_d(t)]^T$. In other words, we establish the correspondence

$$\boldsymbol{w}_d(t) \mapsto [\boldsymbol{x}_d(t), \boldsymbol{u}_d(t)] \tag{7}$$

Using the correspondence (7), we can rewrite Eq. (5) in the following form:

$$\Delta \dot{\boldsymbol{x}} = \boldsymbol{A}_d[\boldsymbol{w}_d(t)]\Delta \boldsymbol{x} + \boldsymbol{B}_d[\boldsymbol{w}_d(t)]\Delta \boldsymbol{u}, \qquad \Delta \boldsymbol{x}(0) = \Delta \boldsymbol{x}_0 \tag{8a}$$

$$\Delta \boldsymbol{y} = \boldsymbol{C}\Delta \boldsymbol{x} \tag{8b}$$

Obviously, the determination of matrices $\boldsymbol{A}_d(\cdot)$ and $\boldsymbol{B}_d(\cdot)$ would in any case require the solution of Problem 1, but the fact that they depend at each time t only on $\boldsymbol{w}_d(t)$ allows us to assume $\boldsymbol{w}_d(t)$ as a scheduling variable and design the feedback controller by using a gain-scheduling approach.

With regard to the choice of the feedback control design technique, we must take into account that the state vector of the linearized model is not completely available because only $\boldsymbol{y}_d(t)$ can be easily computed online. Therefore we propose to use an instantaneous output feedback control law of the form

$$\boldsymbol{u}_{fb}(t) = \boldsymbol{K}[\boldsymbol{w}_d(t)]\Delta \boldsymbol{y}(t) \tag{9}$$

using the following design procedure.

1) Assume $\boldsymbol{w}_d(0) \in \mathcal{W}_0$ and use Eq. (3) to get an estimate of the subset $\mathcal{W} \subset \mathbb{R}^2$ in which, for all $t \in [0, t_f]$, $\boldsymbol{w}_d(t)$ takes determined values. This subset will also contain the nominal speed vector trajectory $\boldsymbol{w}_n(\cdot) = [v_n(\cdot) \quad \gamma_n(\cdot)]^T$.

2) Following the same guidelines that lead to Eq. (7), given the nominal control $\boldsymbol{u}_n(\cdot)$ and the corresponding nominal state trajectory $\boldsymbol{x}_n(\cdot)$ obtained by solving Problem 1 and replacing $\boldsymbol{y}_d$ with $\boldsymbol{y}_n$ and $\boldsymbol{w}_0$ with $\boldsymbol{w}_{n0}$, one can establish the correspondence

$$\boldsymbol{w}_n(t) \mapsto [\boldsymbol{x}_n(t), \boldsymbol{u}_n(t)] \tag{10}$$

Correspondingly, we have

$$\boldsymbol{A}_n[\boldsymbol{w}_n(t)] = \tilde{\boldsymbol{A}}_n[\boldsymbol{x}_n(t), \boldsymbol{u}_n(t)] := \left[\frac{\partial \boldsymbol{f}}{\partial \boldsymbol{x}}\right]_{\substack{\boldsymbol{x}=\boldsymbol{x}_n(\cdot) \\ \boldsymbol{u}=\boldsymbol{u}_n(\cdot) \\ \mu=0}} \tag{11a}$$

$$\boldsymbol{B}_n[\boldsymbol{w}_n(t)] = \tilde{\boldsymbol{B}}_n[\boldsymbol{x}_n(t), \boldsymbol{u}_n(t)] := \left[\frac{\partial \boldsymbol{f}}{\partial \boldsymbol{u}}\right]_{\substack{\boldsymbol{x}=\boldsymbol{x}_n(\cdot) \\ \boldsymbol{u}=\boldsymbol{u}_n(\cdot) \\ \mu=0}} \tag{11b}$$

then a number r of points $\boldsymbol{w}_i = \boldsymbol{w}_n(t_i) \in \mathcal{W}$, $i = 1, \ldots, r$, are selected and the corresponding pairs of matrices $[\boldsymbol{A}_n(\boldsymbol{w}_i), \boldsymbol{B}_n(\boldsymbol{w}_i)]$ are computed.

3) For each triple $[\boldsymbol{A}_n(\boldsymbol{w}_i), \boldsymbol{B}_n(\boldsymbol{w}_i), \boldsymbol{C}]$ a constant gain output feedback linear quadratic (LQ) regulator $\boldsymbol{K}(\boldsymbol{w}_i)$ is designed, according to the procedure developed in Ref. 8, so as to minimize a performance index in the form

$$J = \int_0^{+\infty} (\Delta \boldsymbol{y}^T \tilde{\boldsymbol{Q}}\, \Delta \boldsymbol{y} + \Delta \boldsymbol{u}^T \tilde{\boldsymbol{R}} \Delta \boldsymbol{u})\, \mathrm{d}t \tag{12}$$

where $\tilde{\boldsymbol{Q}}$ and $\tilde{\boldsymbol{R}}$ are suitable weighting matrices. We remember that the convergence of the optimization procedure,[8] which involves the solution of a coupled Riccati equation, is guaranteed provided that an initial stabilizing gain is given.

4) The region $\mathcal{W}$ is partitioned as

$$\mathcal{W} = \bigcup_{i=1}^{r} \mathcal{W}_i \tag{13}$$

with $\mathcal{W}_i$ a suitable region surrounding $\boldsymbol{w}_i$, and a mapping

$$\boldsymbol{w} \in \mathcal{W}_i \mapsto \boldsymbol{K}(\boldsymbol{w}) = \boldsymbol{K}(\boldsymbol{w}_i) \tag{14}$$

is established.

Notice that the closed-loop nominal matrix $\boldsymbol{A}_{\mathrm{CL}n}(t) := \boldsymbol{A}_n[\boldsymbol{w}_n(t)] + \boldsymbol{B}_n[\boldsymbol{w}_n(t)]\boldsymbol{K}[\boldsymbol{w}_n(t)]\boldsymbol{C}$ is, in general, discontinuous at the switching instants. Therefore we slightly modify the control gain $\boldsymbol{K}[\boldsymbol{w}_n(\cdot)]$ in such a way that the switch between $\boldsymbol{K}(\boldsymbol{w}_i)$ and $\boldsymbol{K}(\boldsymbol{w}_{i+1})$ follows a linear function of time; this renders $\boldsymbol{A}_{\mathrm{CL}n}(\cdot)$ continuous in $[0, t_f]$. Moreover, note that, following the design procedure, a sequence of infinite time LQ regulators for time-invariant plants is used to solve a finite time regulation problem for a time-varying plant. A robustness analysis will then be mandatory. Before this, however, note that the use of LQ regulators guarantees that

$$\begin{aligned} \boldsymbol{A}_{\mathrm{CL}n}(t_i) &= \boldsymbol{A}_n[\boldsymbol{w}_n(t_i)] + \boldsymbol{B}_n[\boldsymbol{w}_n(t_i)]\boldsymbol{K}[\boldsymbol{w}_n(t_i)]\boldsymbol{C} \\ &= \boldsymbol{A}_n(\boldsymbol{w}_i) + \boldsymbol{B}_n(\boldsymbol{w}_i)\boldsymbol{K}(\boldsymbol{w}_i)\boldsymbol{C} \end{aligned} \tag{15}$$

has, for all $i = 1, \ldots, r$, all eigenvalues in the left-half of the complex plane. For robustness requirements, which will be clarified in the next section, we make the following stronger assumption.

Assumption 1: $\boldsymbol{A}_{\mathrm{CL}n}(t)$ has all eigenvalues in the left-half of the complex plane for all $t \in [0, t_f]$.

Obviously the truthfulness of this assumption, which is quite reasonable for a large r, can only be checked a posteriori, once the feedback controller has been designed.

IV. Robustness Analysis of the Closed-Loop System

Gain-scheduling controllers[9] have some drawbacks. One is the lack of general results about the stability and the performance analysis of the controlled system. As an alternative to recent techniques proposed in literature (see Ref. 10 and the bibliography therein) based on the $\mathcal{H}_\infty$ approach, in this section we analyze the robustness of the closed-loop system by means of a Lyapunov-based technique.

First note that in our problem a classical stability analysis over an infinite time interval is not necessary because it is only required to have good performances over a finite interval of time. As a consequence, only a practical stability robustness analysis is carried out to give insight into the time behavior of the output tracking error and on the maximum allowable amplitude of impulsive disturbances.

In particular, the following analysis problem is considered. Let $\boldsymbol{w}_0$ be any one of the possible initial speed vector, $\boldsymbol{y}_d(\cdot)$ the corresponding desired output trajectory, and $\boldsymbol{x}_d(\cdot)$ the desired state trajectory solution of the associated Problem 1. Let us denote by $\Delta \boldsymbol{c}(t) := \boldsymbol{c}(t) - \boldsymbol{c}_d(t) = [s(t) - s_d(t) \quad z(t) - z_d(t)]^T$ the difference between the actual and the desired center-of-gravity coordinates. We will analyze the time behavior of the Euclidean norm of $\Delta \boldsymbol{c}(t)$ when an instantaneous state offset $\Delta \boldsymbol{x}_0$ occurs.

Under the feedback control law $\boldsymbol{u}_{fb}(\cdot)$, and taking into account the offset in the initial state, the error model (8) becomes

$$\Delta \dot{\boldsymbol{x}} = \boldsymbol{A}_d[\boldsymbol{w}_d(t)]\Delta \boldsymbol{x} + \boldsymbol{B}_d[\boldsymbol{w}_d(t)]\boldsymbol{u}_{fb}, \qquad \Delta \boldsymbol{x}(0) = \Delta \boldsymbol{x}_0 \tag{16a}$$

$$\Delta \boldsymbol{y} = \boldsymbol{C}\Delta \boldsymbol{x} \tag{16b}$$

$$\Delta \boldsymbol{c} = \boldsymbol{H}\Delta \boldsymbol{x} \tag{16c}$$

where $\boldsymbol{H} = (\boldsymbol{O} \quad \boldsymbol{I}_2)$.

Since

$$\boldsymbol{u}_{fb}(t) = \boldsymbol{K}[\boldsymbol{w}_d(t)]\boldsymbol{C}\Delta \boldsymbol{x} \tag{17}$$

letting

$$\Delta \boldsymbol{A}(t, \boldsymbol{w}_0) = \boldsymbol{A}_d[\boldsymbol{w}_d(t)] - \boldsymbol{A}_n[\boldsymbol{w}_n(t)] \tag{18a}$$

$$\Delta \boldsymbol{B}(t, \boldsymbol{w}_0) = \boldsymbol{B}_d[\boldsymbol{w}_d(t)] - \boldsymbol{B}_n[\boldsymbol{w}_n(t)] \tag{18b}$$

$$\Delta \boldsymbol{K}(t, \boldsymbol{w}_0) = \boldsymbol{K}[\boldsymbol{w}_d(t)] - \boldsymbol{K}[\boldsymbol{w}_n(t)] \tag{18c}$$

where we have taken into account that $\boldsymbol{w}_d(t)$ depends only on t and $\boldsymbol{w}_0$, we can rewrite Eq. (16a) as

$$\dot{\Delta \boldsymbol{x}} = [\boldsymbol{A}_{\mathrm{CL}n}(t) + \boldsymbol{\Delta}(t, \boldsymbol{w}_0)]\Delta \boldsymbol{x} \tag{19}$$

where

$$\boldsymbol{A}_{\mathrm{CL}n}(t) = \boldsymbol{A}_n[\boldsymbol{w}_n(t)] + \boldsymbol{B}_n[\boldsymbol{w}_n(t)]\boldsymbol{K}[\boldsymbol{w}_n(t)]\boldsymbol{C} \tag{20a}$$

$$\boldsymbol{\Delta}(t, \boldsymbol{w}_0) = \Delta \boldsymbol{A}(t, \boldsymbol{w}_0) + \{\boldsymbol{B}_n[\boldsymbol{w}_n(t)]\Delta \boldsymbol{K}(t, \boldsymbol{w}_0) + \Delta \boldsymbol{B}(t, \boldsymbol{w}_0)\boldsymbol{K}[\boldsymbol{w}_n(t)] + \Delta \boldsymbol{B}(t, \boldsymbol{w}_0)\Delta \boldsymbol{K}(t, \boldsymbol{w}_0)\}\boldsymbol{C} \tag{20b}$$

Note that by virtue of Assumption 1 $\boldsymbol{A}_{\mathrm{CL}n}(t)$ in Eq. (19) has all of its eigenvalues in the left-half of the complex plane for all $t \in [0, t_f]$.

To give an estimate of the time behavior of $\|\Delta \boldsymbol{x}\|$ and hence of $\|\Delta \boldsymbol{c}\|$, we used a technique derived from the frozen-time approach proposed in Ref. 6 in the Lyapunov stability setting.

For all $t \in [0, t_f]$, let $\boldsymbol{P}(t)$ be the solution of the Lyapunov equation

$$\boldsymbol{A}_{\mathrm{CL}n}^T(t)\boldsymbol{P}(t) + \boldsymbol{P}(t)\boldsymbol{A}_{\mathrm{CL}n}(t) = -\boldsymbol{N} \tag{21}$$

with $\boldsymbol{N}$ positive definite. The existence, uniqueness, and positive definiteness of $\boldsymbol{P}(t)$ is guaranteed from Assumption 1.

Now let

$$\boldsymbol{\Sigma}(t, \boldsymbol{w}_0) := \dot{\boldsymbol{P}}(t) + \boldsymbol{\Delta}^T(t, \boldsymbol{w}_0)\boldsymbol{P}(t) + \boldsymbol{P}(t)\boldsymbol{\Delta}(t, \boldsymbol{w}_0) - \boldsymbol{N} \tag{22}$$

note that $\boldsymbol{\Sigma}(\cdot, \boldsymbol{w}_0)$ is, in general, discontinuous. Because $\boldsymbol{A}_{\mathrm{CL}n}(\cdot)$ is continuous, however, $\boldsymbol{P}(\cdot)$ is continuous; therefore at a given t the derivative of $\boldsymbol{P}(t)$ and hence $\boldsymbol{\Sigma}(t, \boldsymbol{w}_0)$ can have, at most, first-kind discontinuities. We denote by $\boldsymbol{\Sigma}(t^-, \boldsymbol{w}_0)$ and $\boldsymbol{\Sigma}(t^+, \boldsymbol{w}_0)$ the left and right limits at t, respectively. Define the scalar functions

$$\eta(t, \boldsymbol{w}_0) := \max\left\{\lambda_{\max}\left[\boldsymbol{\Sigma}\left(t^-, \boldsymbol{w}_0\right)\right], \lambda_{\max}\left[\boldsymbol{\Sigma}\left(t^+, \boldsymbol{w}_0\right)\right]\right\} \tag{23}$$

$$\beta(t, \boldsymbol{w}_0) := \begin{cases} \lambda_{\min}[\boldsymbol{P}(t)] & \text{if } \eta(t, \boldsymbol{w}_0) \geq 0 \\ \lambda_{\max}[\boldsymbol{P}(t)] & \text{otherwise} \end{cases} \tag{24}$$

where $\lambda_{\min}[\cdot]$ and $\lambda_{\max}[\cdot]$ denote the minimum and the maximum eigenvalue of the argument; in Appendix B it is proven that

$$\|\Delta \boldsymbol{x}(t)\| \leq \left[\frac{\lambda_{\max}[\boldsymbol{P}(0)]}{\lambda_{\min}[\boldsymbol{P}(t)]}\right]^{\frac{1}{2}} \exp\left[\frac{1}{2}\int_0^t \frac{\eta(\tau, \boldsymbol{w}_0)}{\beta(\tau, \boldsymbol{w}_0)}\,\mathrm{d}\tau\right]\|\Delta \boldsymbol{x}_0\| \tag{25}$$

which gives an upper bound for $\|\Delta \boldsymbol{x}(t)\|$.

Since $\|\boldsymbol{H}\| = 1$, the same upper bound (25) holds for $\|\Delta \boldsymbol{c}(t)\|$.

The preceding analysis has been carried out for a particular $\boldsymbol{w}_0$. A more conservative estimate of an upper bound for $\|\Delta \boldsymbol{c}(\cdot)\|$ can be obtained by maximizing the function $\eta(t, \boldsymbol{w}_0)$ for each t, with respect to $\boldsymbol{w}_0$:

$$\hat{\eta}(t) := \max_{\boldsymbol{w}_0 \in \mathcal{W}_0} \eta(t, \boldsymbol{w}_0), \qquad \forall t \in [0, t_f] \tag{26}$$

correspondingly, we define

$$\hat{\beta}(t) := \begin{cases} \lambda_{\min}[\boldsymbol{P}(t)] & \text{if } \hat{\eta}(t) \geq 0 \\ \lambda_{\max}[\boldsymbol{P}(t)] & \text{otherwise} \end{cases} \tag{27}$$

In this case the upper bound (25) becomes

$$\|\Delta \boldsymbol{c}(t)\| \leq \left[\frac{\lambda_{\max}[\boldsymbol{P}(0)]}{\lambda_{\min}[\boldsymbol{P}(t)]}\right]^{\frac{1}{2}} \times \exp\left[\frac{1}{2}\int_0^t \frac{\hat{\eta}(\tau)}{\hat{\beta}(\tau)}\,\mathrm{d}\tau\right]\|\Delta \boldsymbol{x}_0\| := \overline{\Delta c}(t)\|\Delta \boldsymbol{x}_0\| \tag{28}$$

and holds for any initial speed vector $\boldsymbol{w}_0 \in \mathcal{W}_0$.

Knowing $\overline{\Delta c}(t)$ enables us to evaluate, according to Eq. (6), the maximum value $\|[\Delta\alpha(0) \;\; \Delta q(0)]^T\|_{\max}$ of the initial state displacement and the maximum value $d_{\max}$ of $\|\boldsymbol{d}\|$ guaranteeing, for all $t \in [0, t_f]$, $\|\Delta \boldsymbol{c}(t)\| \leq M$. If the impulsive disturbance occurs at a time $\tilde{t} \neq 0$, Eq. (28) is still valid for $t \in [\tilde{t}, t_f]$ replacing $\Delta \boldsymbol{x}_0$ with $\Delta \boldsymbol{x}(\tilde{t})$ and 0 with $\tilde{t}$ in Eq. (6a).

V. Simulation Results

The control strategy described in the preceding sections has been tested in simulation with reference to the RPV MIRACH 100 manufactured by METEOR. The main physical and geometrical parameter values of this aircraft are

$$m = 230\,\mathrm{kg} \qquad S = 0.82\,\mathrm{m}^2 \qquad c = 0.476\,\mathrm{m}$$

$$I_y = 2630\,\mathrm{kgm}^2 \qquad A = 2.96 \qquad M = 0.25\,\mathrm{m}$$

As far as the aerodynamic data are concerned, by interpolating tables of wind-tunnel data, the coefficients C_L and C_m were assumed linearly dependent on α_a, q, and δ_e,

$$C_L = C_{L0} + C_{L\alpha}\alpha + C_{Lq}(qc/2v) + C_{L\delta_e}\delta_e \tag{29}$$

$$C_m = C_{m0} + C_{m\alpha}\alpha + C_{mq}(qc/2v) + C_{m\delta_e}\delta_e \tag{30}$$

whereas the coefficient C_D was calculated as

$$C_D = C_{D0} + C_L^2/(\pi A)$$

The values of the stability derivatives are given as

$$C_{L0} = 0.1660 \qquad C_{L\alpha} = 5.007 \qquad C_{Lq} = 11.14$$

$$C_{L\delta_e} = 0.9700 \qquad C_{m0} = 0.0956 \qquad C_{m\alpha} = -1.313 \tag{31}$$

$$C_{mq} = -20.58 \qquad C_{m\delta_e} = -2.940 \qquad C_{D0} = 0.0445$$

Finally, the air density ρ was set to $\rho = 1.014\ \mathrm{kg/m}^3$ (corresponding to the air density at an altitude of 2200 m according to the International Standard Atmosphere).

Based on an analysis of the pull-up maneuver,[1] a nominal initial speed vector $\boldsymbol{w}_{n0} = (v_{n0} \;\; \gamma_{n0})^T = (176\ \mathrm{m/s} \;\; 56.0\ \mathrm{deg})^T$ was assumed, whereas the uncertainty region $\mathcal{W}_0$ was defined as

$$\mathcal{W}_0 := \left\{(v_0 \quad \gamma_0)^T : |v_0 - v_{n0}| < \Delta v_0, |\gamma_0 - \gamma_{n0}| < \Delta\gamma_0\right\} \tag{32}$$

with $\Delta v_0 = 2$ m/s and $\Delta\gamma_0 = 1$ deg.

A. Controller Design

For the design of the control law a time duration of the parabolic flight of 30 s was assumed.

First, on the basis of the nominal inital speed vector $\boldsymbol{w}_{n0}$, the nominal control $\boldsymbol{u}_n(\cdot)$ was determined as the solution of Problem 1, in which the weighting matrices were set to

$$\boldsymbol{Q} = \boldsymbol{I}_2 \qquad \boldsymbol{R} = 10^{-8}\boldsymbol{I}_2 \tag{33}$$

The time history of $\boldsymbol{u}_n(\cdot)$ and the related position-tracking errors $\boldsymbol{e}_y = (e_{y_1} \;\; e_{y_2})^T$ are shown in Fig. 1.

Next, for a given initial speed vector $\boldsymbol{w}_0 = (174 \;\; 55)^T$, Problem 1 was solved offline via classical nonlinear programming techniques, and the corresponding optimal control $\boldsymbol{u}_d(\cdot)$ was determined. As already stated, these techniques are computationally cumbersome and cannot be used online; therefore, via the algorithm described in Appendix A, we evaluated an approximation of the optimal control law, say $\tilde{\boldsymbol{u}}(\cdot)$. Figures 2a and 2b, comparing $\boldsymbol{u}_d(\cdot)$ with $\tilde{\boldsymbol{u}}_d(\cdot)$, show that the difference $\tilde{\boldsymbol{u}}(t) - \boldsymbol{u}_d(t)$ is kept small during the parabola.

Note that since the initial speed vector differs slightly from the nominal one an approximation of $\boldsymbol{u}_d(\cdot)$ could be $\boldsymbol{u}_n(\cdot)$, solution of Problem 1 in correspondence with the nominal speed vector $\boldsymbol{w}_{n0}$. In practice, numerical simulations referenced to the RPV show that $\tilde{\boldsymbol{u}}$ is a much better approximation than $\boldsymbol{u}_n$ (see Figs. 2c and 2d).

As far as the feedback gain-scheduled controller design is concerned, the region $\mathcal{W}$ of possible values of the gain-scheduling variables v and γ was determined by using Eq. (3) for various values

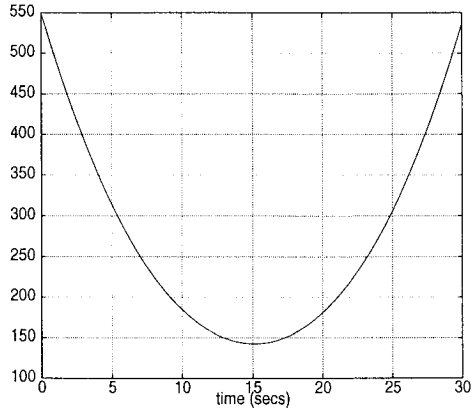

Fig. 1a Thrust (N).

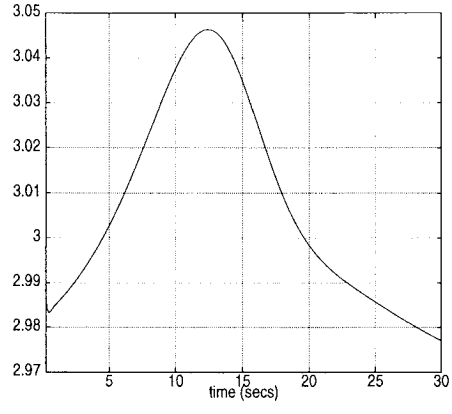

Fig. 1b Elevator deflection (deg).

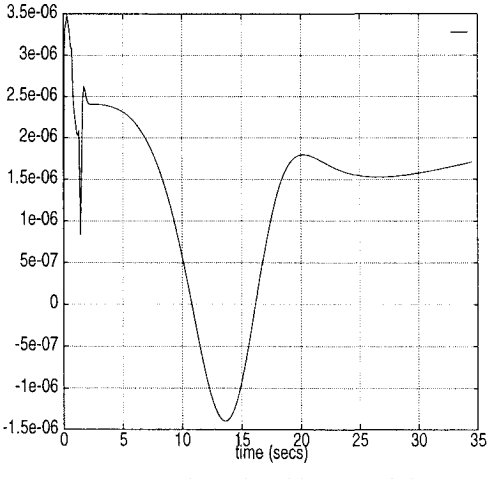

Fig. 1c Horizontal position error (m).

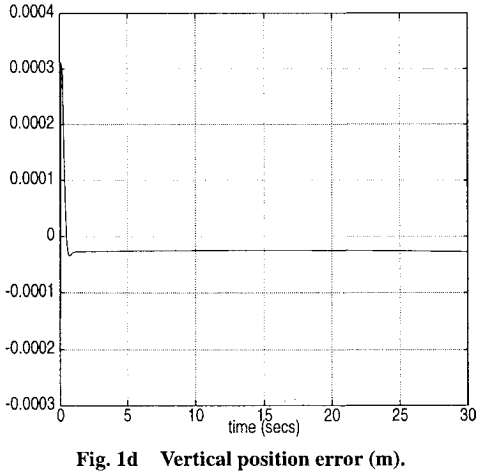

Fig. 1d Vertical position error (m).

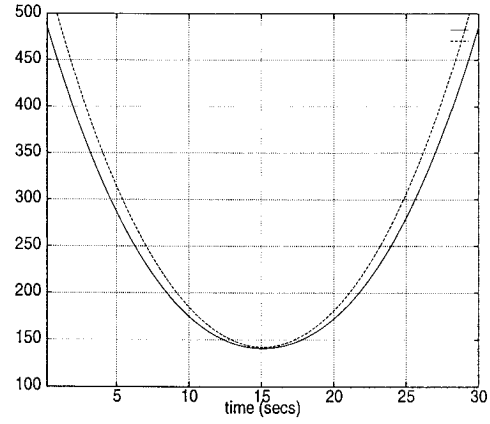

Fig. 2a Thrust (N): ——, $u_d(\cdot)$ and ....., $\tilde{u}(\cdot)$.

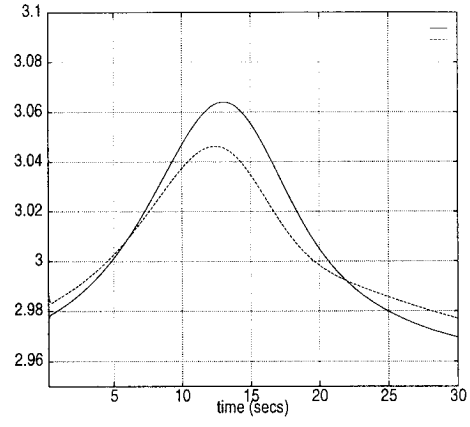

Fig. 2b Elevator deflection (deg): ——, $u_d(\cdot)$ and ....., $\tilde{u}(\cdot)$.

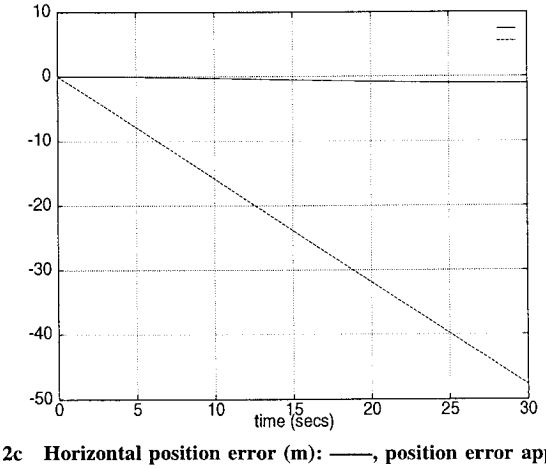

Fig. 2c Horizontal position error (m): ——, position error applying $\tilde{u}(\cdot)$ and ....., position error applying u_n.

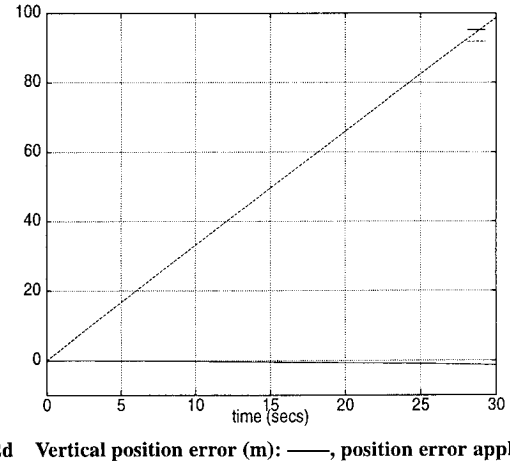

Fig. 2d Vertical position error (m): ——, position error applying $\tilde{u}(\cdot)$ and ....., position error applying u_n.

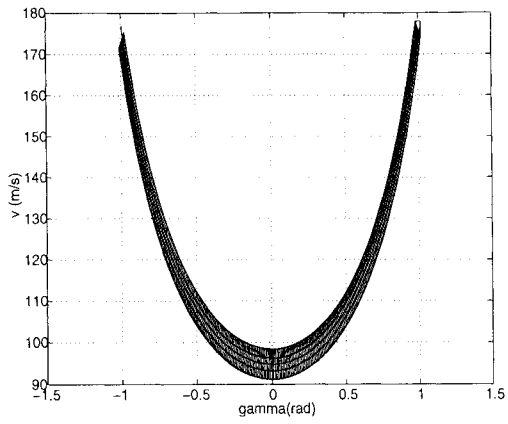

Fig. 3a Region $\mathcal{W}$ and its partitioning.

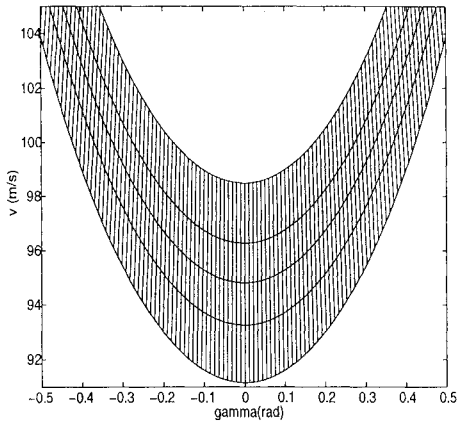

Fig. 3b Zoom on the middle part of region $\mathcal{W}$.

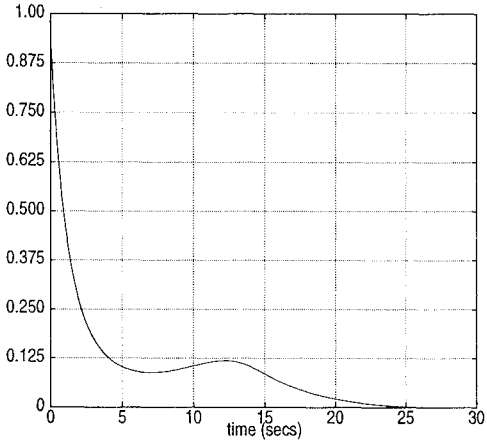

Fig. 4a Plot of $\overline{\Delta c(t)}$.

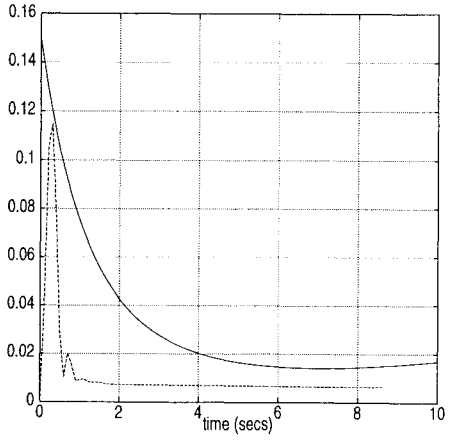

Fig. 4b Bound compared with simulation result.

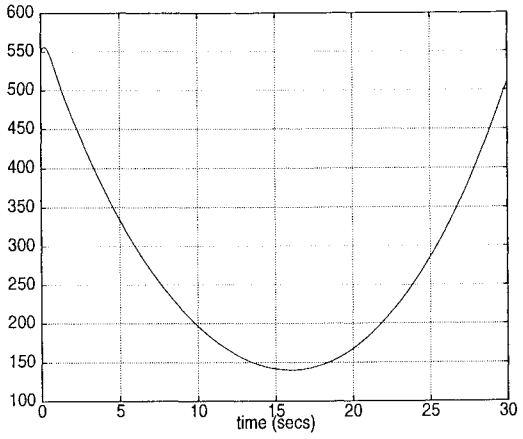

Fig. 5a Thrust (N).

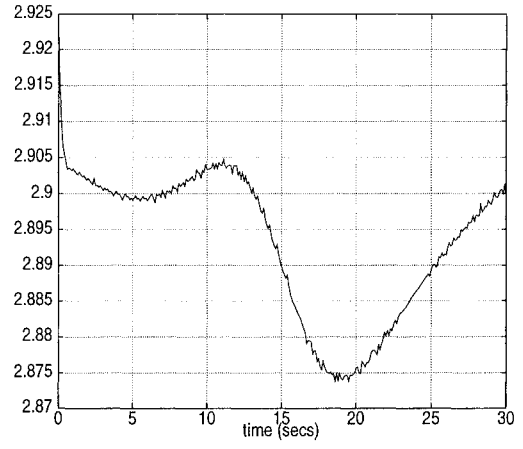

Fig. 5b Elevator deflection (deg).

$\boldsymbol{w}_0 \in \mathcal{W}_0$. Then 300 points $\boldsymbol{w}_i$ uniformly distributed on the nominal speed vector trajectory $\boldsymbol{w}_n(\cdot)$ were chosen and, correspondingly, a partition of the region $\mathcal{W}$ was selected; the partition is shown in Fig. 3. For each $\boldsymbol{w}_i$ the matrices $\boldsymbol{A}(\boldsymbol{w}_i)$ and $\boldsymbol{B}(\boldsymbol{w}_i)$ were determined, and the output gain matrix $\boldsymbol{K}(\boldsymbol{w}_i)$, minimizing the performance index (12), was calculated assuming $\bar{\boldsymbol{Q}} = \boldsymbol{I}_2$ and $\bar{\boldsymbol{R}} = \text{diag}(10^4, 10^{-4})$; to this end we used the MATLAB Toolbox.[11] Finally the truthfulness of Assumption 1 was checked.

B. Robustness Analysis

To determine the upper bound for $\|\Delta \boldsymbol{c}(t)\|$ as given by Eq. (28), first we have to choose the right-hand side in the Lyapunov equation (21). Since the bound strongly depends on the ratio between the maximum and minimum eigenvalue of $\boldsymbol{P}(\cdot)$, a choice for $\boldsymbol{N}$ that yields a well-conditioned matrix function $\boldsymbol{P}(\cdot)$ is necessary. If $\boldsymbol{A}_{\text{CL}n}(\cdot)$ was well balanced, a reasonable $\boldsymbol{N}$ could be the identity matrix; however, this is not our case because of the different orders of magnitude of the components of the state vector. Therefore, let $\boldsymbol{T}$ be the balancing matrix of $\boldsymbol{A}_{\text{CL}n}(0)$ and $\hat{\boldsymbol{A}}_{\text{CL}n}(t) = \boldsymbol{T}\boldsymbol{A}_{\text{CL}n}(t)\boldsymbol{T}^{-1}$. Let $\hat{\boldsymbol{P}}(\cdot)$ be the solution of the Lyapunov equation

$$\hat{\boldsymbol{A}}^{T}_{\text{CL}n}(t)\,\hat{\boldsymbol{P}}(t) + \hat{\boldsymbol{P}}(t)\,\hat{\boldsymbol{A}}_{\text{CL}n}(t) = -\boldsymbol{I} \tag{34}$$

Premultiplying Eq. (34) by $\boldsymbol{T}^T$ and postmultiplying by $\boldsymbol{T}$ and letting $\boldsymbol{P}(t) = \boldsymbol{T}^T\hat{\boldsymbol{P}}(t)\boldsymbol{T}$, we get the Lyapunov equation (21) with $\boldsymbol{N} = \boldsymbol{T}^T\boldsymbol{T}$, which is our choice of $\boldsymbol{N}$.

For the evaluation of the function $\hat{\eta}(t)$ given by Eq. (26), 100 points $\boldsymbol{w}_0$, uniformly distributed in $\mathcal{W}_0$, were chosen. For each of them, the function $\boldsymbol{\Delta}(t, \boldsymbol{w}_0)$ was determined with a time step of 0.1 s, the same step used for the calculation of $\boldsymbol{P}(t)$ and $\dot{\boldsymbol{P}}(t)$. All of these calculations were achieved via an efficient software tool developed at CIRA in the MATLAB environment.

The function $\overline{\Delta c}(\cdot)$ defined in Eq. (28) was finally calculated and is shown in Fig. 4a. From this calculation it follows that, to guarantee $\|\Delta \boldsymbol{c}(t)\| \leq M = 0.25$ m, a maximum displacement $\|[\Delta\alpha(0) \;\; \Delta q(0)]^T\|_{\max} = 0.25$ or an impulsive disturbance at $t = 0$ with a maximum amplitude $d_{\max} = 1.5$ m (which corresponds to a horizontal wind gust of 15 m/s and duration of 0.1 s) can be tolerated.

The weak conservativeness of this estimate can be seen in Fig. 4b, where the time history of $\|\Delta \boldsymbol{c}(\cdot)\|$ is shown for the case of a horizontal wind gust at $t = 0$ of 10-m/s intensity and 0.1-s duration compared with $\overline{\Delta c}(t)\tilde{\boldsymbol{B}}_\mu(0)$. Finally, Fig. 5 shows the time histories of the overall control inputs.

VI. Conclusions

An automatic flight controller for parabolic flights of a remotely piloted vehicle was designed. The control law consisted of a feedforward part, designed around the trajectory to be tracked in the absence of external disturbances, and of a feedback term. The latter employed constant gain output feedback matrices that are gain-scheduled with the speed vector along the desired trajectory. A performance analysis was carried out to determine an upper bound of the norm of the tracking error between the actual and the desired center-of-gravity coordinates.

Appendix A: Solution of Problem 1

To solve Problem 1 we propose a procedure based on the linearization of the nonlinear model (1) around the nominal trajectory $\boldsymbol{x}_n(\cdot)$, $\boldsymbol{u}_n(\cdot)$, which because of its simplicity can be implemented online and which allows us to evaluate the feedforward control law. Its effectiveness has been confirmed by numerical simulations (see Sec. V).

By linearizing the nonlinear model(1) around the nominal trajectory $\boldsymbol{x}_n(t), \boldsymbol{u}_n(t)$, a suboptimal solution of Problem 1 can be obtained by solving Problem 2.

Problem 2:

$$\min_{\Delta \boldsymbol{u}(\cdot)_{[0,t_f]}, \Delta\alpha_0, \Delta q_0} \int_0^{t_f} \left(\boldsymbol{e}_{\Delta y}^T \boldsymbol{Q} \boldsymbol{e}_{\Delta y} + \Delta \boldsymbol{u}^T \boldsymbol{R} \Delta \boldsymbol{u}\right) dt$$

subject to

$$\Delta \dot{\boldsymbol{x}} = \left[\frac{\partial \boldsymbol{f}}{\partial \boldsymbol{x}}\right]_{\substack{x=x_{n(\cdot)} \\ u=u_{n(\cdot)} \\ \mu=0}} \Delta \boldsymbol{x} + \left[\frac{\partial \boldsymbol{f}}{\partial \boldsymbol{u}}\right]_{\substack{x=x_{n(\cdot)} \\ u=u_{n(\cdot)} \\ \mu=0}} \Delta \boldsymbol{u}$$

$$:= \boldsymbol{A}_n(t)\Delta \boldsymbol{x} + \boldsymbol{B}_n(t)\Delta \boldsymbol{u}, \quad \Delta \boldsymbol{x}(0) = [\Delta\alpha_0 \;\; \Delta q_0 \;\; \Delta y(0)]^T \tag{A1a}$$

$$\Delta \boldsymbol{y} = \boldsymbol{C}\Delta \boldsymbol{x} \tag{A1b}$$

where, since we linearize around $\boldsymbol{x}_n(\cdot)$ and $\boldsymbol{u}_n(\cdot)$, $\Delta \boldsymbol{y} = \boldsymbol{y} - \boldsymbol{y}_n$ and $\Delta \boldsymbol{u} = \boldsymbol{u} - \boldsymbol{u}_n$; moreover let $\boldsymbol{e}_{\Delta y} := \Delta \boldsymbol{y} - \Delta \boldsymbol{y}_d$ and $\Delta \boldsymbol{y}_d := \boldsymbol{y}_d - \boldsymbol{y}_n$. Note that $\boldsymbol{e}_{\Delta y} = \boldsymbol{y} - \boldsymbol{y}_d$.

On the other hand, system (A1), for any given pair $(\Delta\alpha_0 \;\; \Delta q_0)^T$, admits a control function $\Delta \boldsymbol{u}$ guaranteeing the perfect output tracking (i.e., $\boldsymbol{e}_{\Delta y}(t) = 0$ for all $t \in [0, t_f]$). This solution can be obtained by solving the linear inversion problem associated with systems (A1a) and (A1b) when $\Delta \boldsymbol{y} = \Delta \boldsymbol{y}_d$ is imposed.

By partitioning the vector $\Delta \boldsymbol{x}$ as $(\Delta\alpha \;\; \Delta q \;\; \Delta y)^T$ and imposing $\Delta \boldsymbol{y} = \Delta \boldsymbol{y}_d$, the linearized model (A1a) can be written as

$$\begin{pmatrix} \Delta\dot{\alpha} \\ \Delta\dot{q} \end{pmatrix} = \boldsymbol{A}_1(t) \begin{pmatrix} \Delta\alpha \\ \Delta q \end{pmatrix} + \boldsymbol{B}_1(t) \begin{pmatrix} \Delta T \\ \Delta\delta_e \end{pmatrix} + \zeta_1(t) \tag{A2a}$$

$$\begin{pmatrix} 0 \\ 0 \end{pmatrix} = \boldsymbol{A}_2(t) \begin{pmatrix} \Delta\alpha \\ \Delta q \end{pmatrix} + \boldsymbol{B}_2(t) \begin{pmatrix} \Delta T \\ \Delta\delta_e \end{pmatrix} + \zeta_2(t) \tag{A2b}$$

$$\Delta\alpha(0) = \Delta\alpha_0 \tag{A2c}$$

$$\Delta q(0) = \Delta q_0 \tag{A2d}$$

where $\zeta_1(\cdot)$ and $\zeta_2(\cdot)$ are known vector functions. The solution of this algebraic-differential equation system gives the desired unknown function $\Delta \boldsymbol{u} = (\Delta T \;\; \Delta\delta_e)^T$.

The numerical techniques to solve Eqs. (A2) are still too cumbersome to be performed online. A further simplification of the problem can be obtained by considering that, in practice, $\Delta\alpha$ exhibits slow time variations during the parabolic flight so that $\Delta\dot{\alpha}(t) \cong 0$ and, from Eqs. (1a) and (1d), $\Delta q(t) \cong \dot{\gamma}_d(t) - \dot{\gamma}_n(t)$.

Finally, coming back to the choice of $\Delta\alpha_0$ and Δq_0, we remark that their values essentially affect the amplitude of the control inputs. A good choice is given by $\Delta\alpha_0 = 0$ and $\Delta q_0 = \dot{\gamma}_{d0} - \dot{\gamma}_{n0}$. In conclusion, the earlier assumptions allow us to reduce the algebraic-differential equation system (A2) to a purely algebraic time-varying system whose solution gives a good approximation of the optimal solution $\Delta \boldsymbol{u}_d$ of Problem 2 whenever the matrix $\boldsymbol{R}$ is sufficiently small [as is our case, see also Eq. (33)].

Appendix B: Proof of Equation (25)

Let us define $v(t, \Delta \boldsymbol{x}) = \Delta \boldsymbol{x}^T \boldsymbol{P}(t) \Delta \boldsymbol{x}$. We have

$$0 < \lambda_{\min}[\boldsymbol{P}(t)]\|\Delta \boldsymbol{x}\|^2 \leq v(t, \Delta \boldsymbol{x}) \leq \lambda_{\max}[\boldsymbol{P}(t)]\|\Delta \boldsymbol{x}\|^2$$

$$\forall t \in [0, t_f] \quad \forall \Delta \boldsymbol{x} \in \mathbb{R}^6 \tag{B1}$$

Since $\boldsymbol{P}(\cdot)$ is not guaranteed to be differentiable in $[0, t_f]$ we introduce the generalized derivative of $v(t, \Delta \boldsymbol{x})$ along the trajectory $\Delta \boldsymbol{x}(\cdot)$ as follows (see Ref. 12):

$$\dot{v}(t, \Delta \boldsymbol{x}) := \limsup_{\Delta t \to 0} \frac{\{\Delta \boldsymbol{x} + \Delta t[\boldsymbol{A}_{\mathrm{CL}n}(t) + \boldsymbol{\Delta}(t, w_0)]\Delta \boldsymbol{x}\}^T \boldsymbol{P}(t + \Delta t)\{\Delta \boldsymbol{x} + \Delta t[\boldsymbol{A}_{\mathrm{CL}n}(t) + \boldsymbol{\Delta}(t, w_0)]\Delta \boldsymbol{x}\} - \Delta \boldsymbol{x}^T \boldsymbol{P}(t)\Delta \boldsymbol{x}}{\Delta t} \tag{B2}$$

Clearly the generalized derivative of v returns the classical derivative at the differentiability points. Recalling Eq. (22), we have

$$\begin{aligned}
\dot{v}(t, \Delta \boldsymbol{x}) = \limsup_{\Delta t \to 0} \Delta \boldsymbol{x}^T \Bigg\{ & \frac{\boldsymbol{P}(t + \Delta t) - \boldsymbol{P}(t)}{\Delta t} \\
& + \boldsymbol{P}(t + \Delta t)[\boldsymbol{A}_{\mathrm{CL}n}(t) + \boldsymbol{\Delta}(t, w_0)] \\
& + [\boldsymbol{A}_{\mathrm{CL}n}(t) + \boldsymbol{\Delta}(t, w_0)]^T \\
& \times \boldsymbol{P}(t + \Delta t) + \Delta t[\boldsymbol{A}_{\mathrm{CL}n}(t) + \boldsymbol{\Delta}(t, w_0)]^T \\
& \times \boldsymbol{P}(t + \Delta t)[\boldsymbol{A}_{\mathrm{CL}n}(t) + \boldsymbol{\Delta}(t, w_0)] \Bigg\} \Delta \boldsymbol{x} \\
\leq \max & \left[\Delta \boldsymbol{x}^T \boldsymbol{\Sigma}\left(t^-, w_0\right)\Delta \boldsymbol{x}, \; \Delta \boldsymbol{x}^T \boldsymbol{\Sigma}\left(t^+, w_0\right)\Delta \boldsymbol{x}\right] \\
\leq \max & \left\{\lambda_{\max}\left[\boldsymbol{\Sigma}\left(t^-, w_0\right)\right]\|\Delta \boldsymbol{x}\|^2, \right. \\
& \left. \lambda_{\max}\left[\boldsymbol{\Sigma}\left(t^+, w_0\right)\right]\|\Delta \boldsymbol{x}\|^2\right\} \\
= \eta & (t, w_0)\|\Delta \boldsymbol{x}\|^2
\end{aligned} \tag{B3}$$

and, therefore,

$$\frac{\dot{v}[t, \Delta \boldsymbol{x}(t)]}{v[t, \Delta \boldsymbol{x}(t)]} \leq \frac{\eta[t, w_0]}{\beta[t, w_0]} \tag{B4}$$

Integrating both sides in Eq. (B4) and using Eq. (B1), we obtain

$$v[t, \Delta \boldsymbol{x}(t)] \leq v(0, \Delta \boldsymbol{x}_0) \exp\left[\int_0^t \frac{\eta(\tau, w_0)}{\beta(\tau, w_0)} d\tau\right] \tag{B5}$$

from which it follows that

$$v[t, \Delta \boldsymbol{x}(t)] \leq \lambda_{\max}[\boldsymbol{P}(0)] \exp\left[\int_0^t \frac{\eta(\tau, w_0)}{\beta(\tau, w_0)} d\tau\right] \|\Delta \boldsymbol{x}_0\|^2 \tag{B6}$$

On the other hand, from Eq. (B1) follows

$$v[t, \Delta \boldsymbol{x}(t)] \geq \lambda_{\min}[\boldsymbol{P}(t)]\|\Delta \boldsymbol{x}(t)\|^2 \tag{B7}$$

Combining Eqs. (B6) and (B7), inequality (25) follows.

References

[1]Mattei, M., "Parabolic Flights for Microgravity Experiments," Centro Italiano Ricerche Aerospaziali, Final Rept. DILC-INT-TN-373, Capua, Italy, Jan. 1994.

[2]Amato, F., Ambrosino, G., Garofalo, F., and Verde, L., "A Flight Control System for Microgravity Experiments," *Proceedings of the 1st IEEE Conference on Control Applications* (Dayton, OH), 1992, pp. 351–353.

[3]Snell, S. A., Enns Dale, F., and Garrard, W. L., "Nonlinear Inversion Flight Control for a Supermaneuverable Aircraft," *Journal of Guidance, Control, and Dynamics*, Vol. 15, No. 4, 1992, pp. 976–984.

[4]Azam, M., and Singh, S. M., "Invertibility and Trajectory Control for Nonlinear Maneuvers of Aircraft," *Journal of Guidance, Control, and Dynamics*, Vol. 17, No. 1, 1994, pp. 192–200.

[5]Monaco, S., and D'Antonio, L., "A Nonlinear Controller for Parabolic Flights," *Proceedings of the 32nd IEEE Conference on Decision and Control* (San Antonio, TX), 1993, pp. 1513–1518.

[6]Amato, F., Celentano, G., and Garofalo, F., "New Sufficient Conditions for the Stability of Slowly-Varying Linear Systems," *IEEE Transactions on Automatic Control*, Vol. AC-38, No. 9, 1993, pp. 1409–1411.

[7]Etkin, B., *Dynamics of Atmospheric Flight*, Wiley, New York, 1972, Chap. 10.

[8]Moerder, D. D., and Calise, A. J., "Convergence of a Numerical Algorithm for Calculating Optimal Output Feedback Gains," *IEEE Transactions on Automatic Control*, Vol. AC-30, No. 9, 1985, pp. 900–903.

[9]Åström, K. J., and Wittenmark, B., *Adaptive Control*, Addison–Wesley, Reading, MA, 1989.

[10]Hyde, R. A., and Glover, K., "The Application of Scheduled $\mathcal{H}_\infty$ Controllers to a VSTOL Aircraft," *IEEE Transactions on Automatic Control*, Vol. AC-38, No. 7, 1993, pp. 1021–1039.

[11]Byrns, E. V. S., "Fixed Order Compensation Toolbox," Version 1.0, Dynamic Systems Consulting, Alexandria, VA, 1993.

[12]Hahn, W., *Stability of Motion*, Springer–Verlag, Heidelberg, 1967, p. 196.